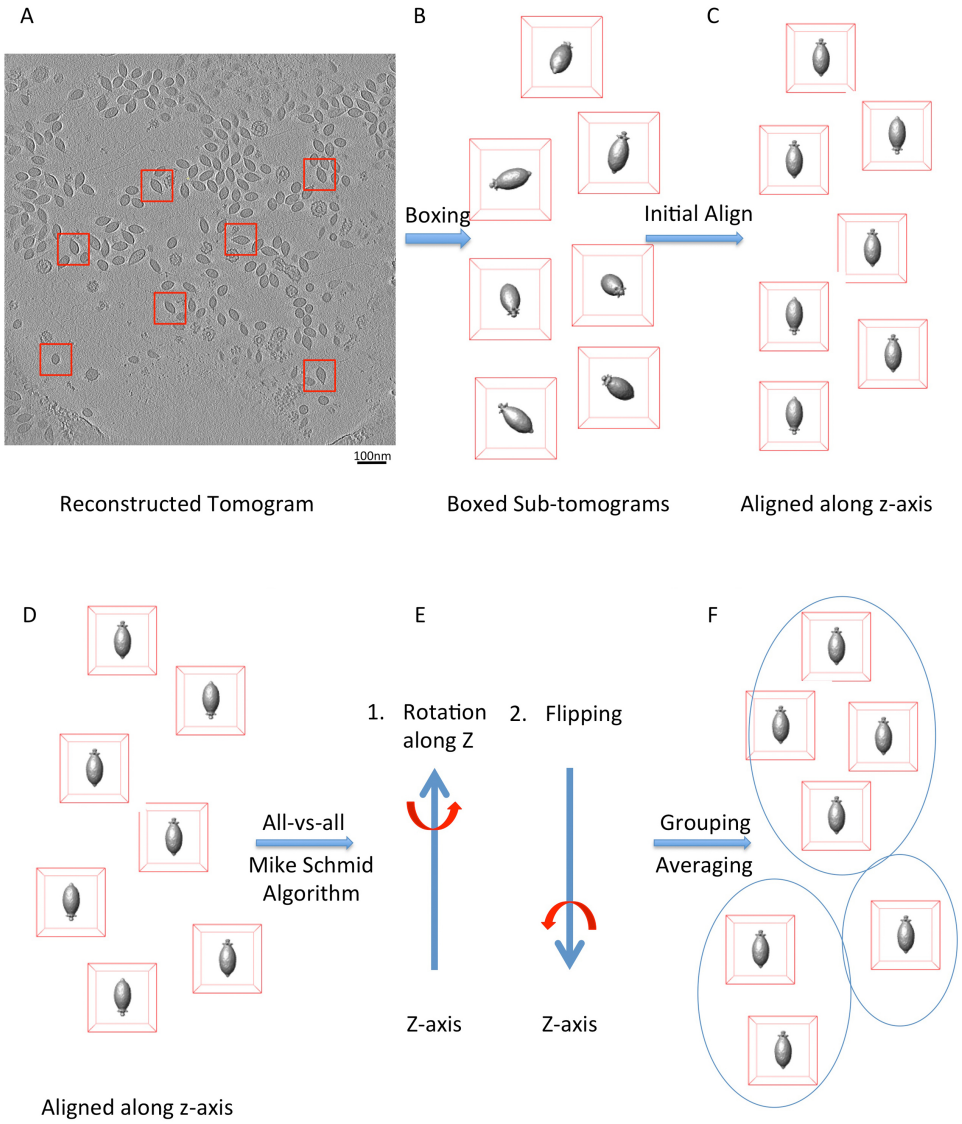

Figure S1. Workflow for the subtomogram alignment and averaging. (A) A representative single slice from a reconstructed tomogram. (B) Computationally-extracted subtomogram particles in cubic boxes. (C) and (D) First-step aligned particles to its long axis (Z-axis). (E) Two comparisons considered in the all-vs-all algorithm: azimuthally rotation along the Z-axis to match the tail spikes and flipping between the two ends to tell which end contains the tail. (F) Grouping and Averaging after all-vs-all comparison to obtain averages from the major group as well as minor groups.

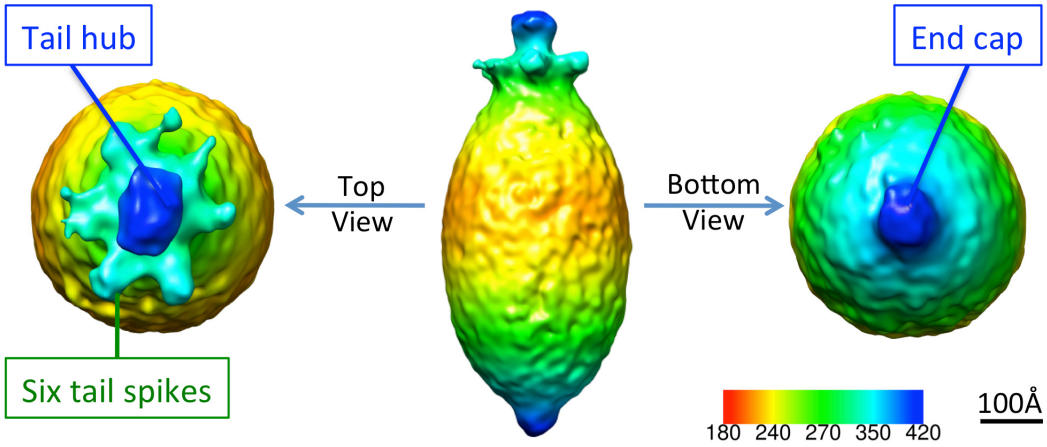

Figure S2. The symmetry-free average of His1 virus generated from 30 subtomograms using model-free all-vs-all alignment method. The map is radially colored with side view (middle), top view (left) and bottom view (right).

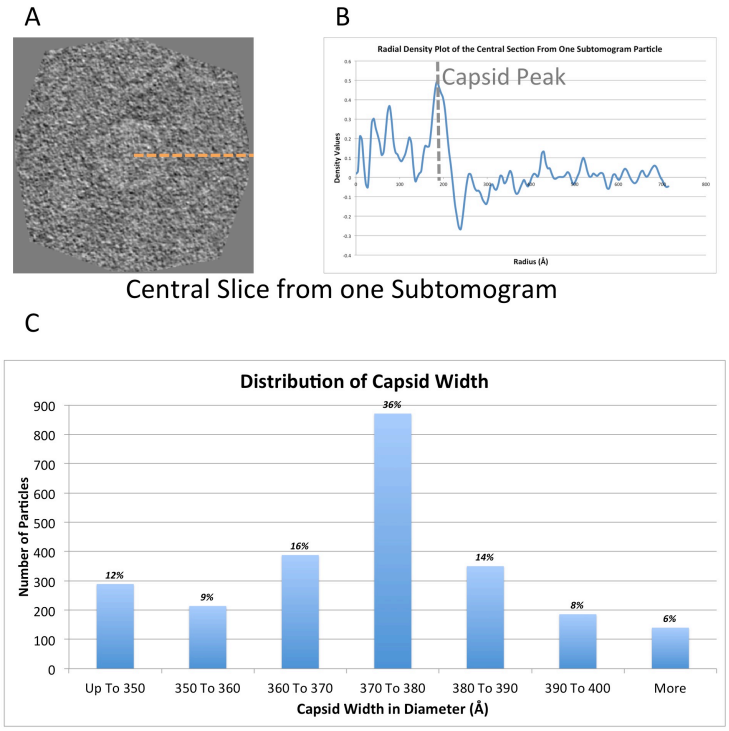

Figure S3. The plot of the distribution of the capsid peak radius for all subtomogram particles indicates that the radius of the capsid tends to have a continuous distribution. (A) The central slice of one representative subtomogram particle. (B) The radial plot of the central slice in (A) and the capsid peak is indicated in grey dashed line. (C) The plot for the distribution for radius of all subtomogram particles.

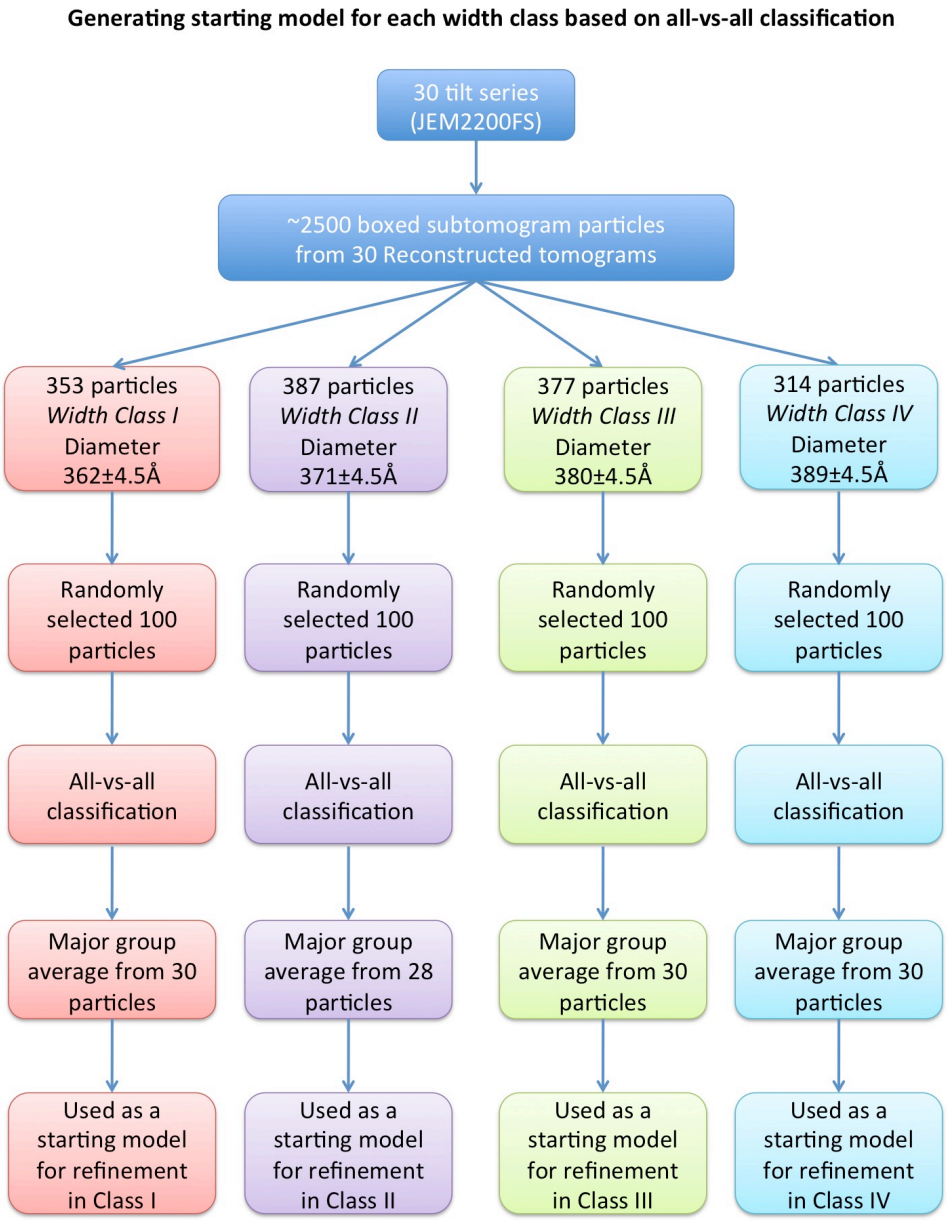

Figure S4. Workflow for generating starting models for each width class through all-vs-all. Subtomogram particles were split based on their width size into Class I (red), Class II (purple), Class III (green), and Class IV (Cyan). The all-vs-all classification was performed within each class to generate an average, which would be used as a starting model for further refinement for particles in each width class.

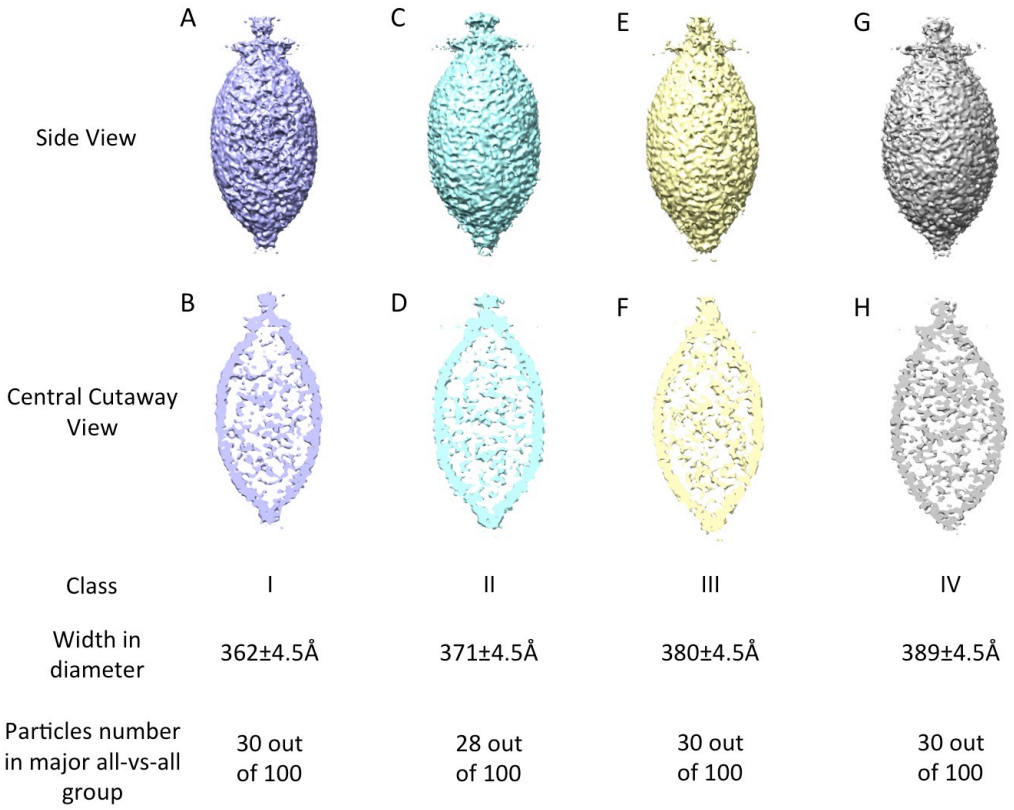

Figure S5. All-vs-all subtomogram averages within different width classes. (A) The side view and (B) the central cutaway view of major group average of Class I (width diameter 362±4.5Å) all-vs-all classification. (C) The side view and (D) the central cutaway view of major group average of Class II (width diameter 371±4.5Å) all-vs-all classification. (E) The side view and (F) the central cutaway view of major group average of Class III (width diameter 380±4.5Å) all-vs-all classification. (G) The side view and (H) the central cutaway view of major group average of Class IV (width diameter 389±4.5Å) all-vs-all classification.

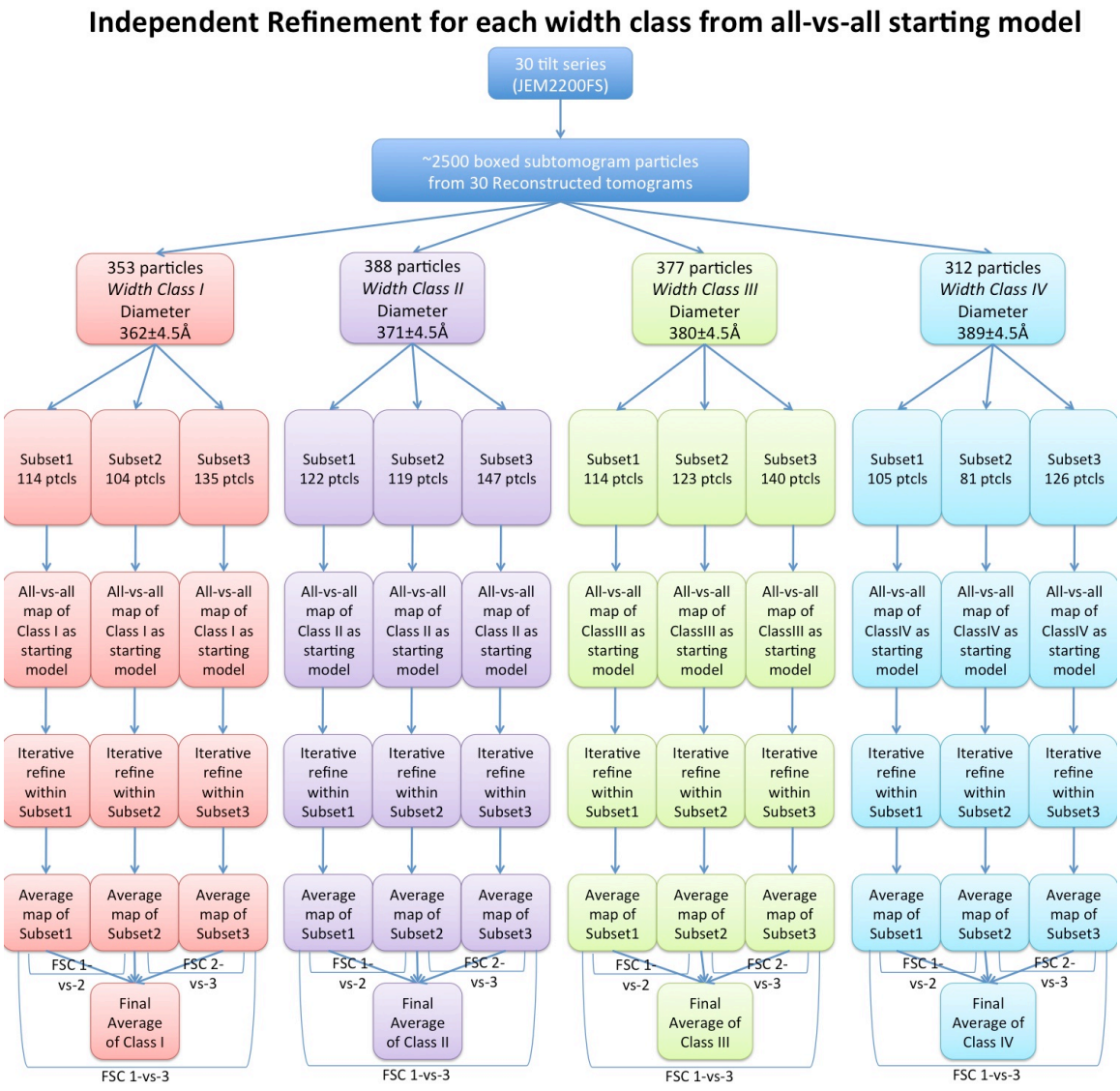

Figure S6. Workflow for independent refinements for each width class. Subtomogram particles were split based on their width size into Class I (red), Class II (purple), Class III (green), and Class IV (Cyan). Within each class, three subsets were further split according to the month tomogram data were collected, namely Subset1, Subset2 and Subset3. For each class, the iterative refinements were done independently within each subset starting form the all-vs-all average. FSCs calculated for each pair of the three subsets were obtained for each width class.

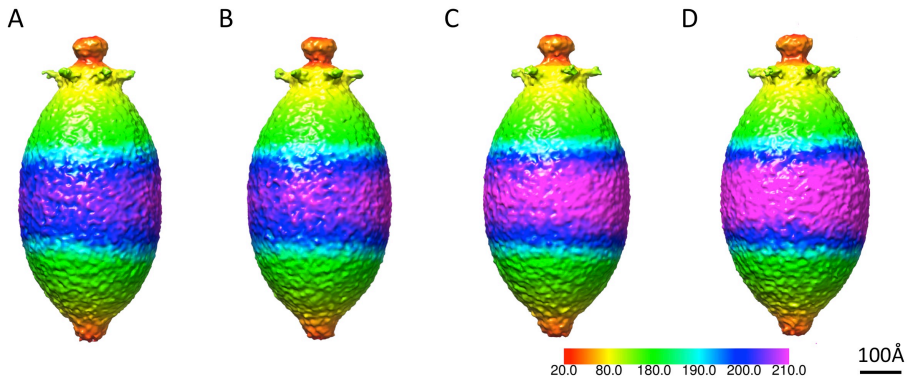

Class	I	II	III	IV
Width in diameter	362±4.5Å	371±4.5Å	380±4.5Å	389±4.5Å
Particles number	353	388	377	312

Figure S7. Subtomogram averages in different width classes (cylinder radially colored). The side views of group average of (A) Class I (width diameter 362±4.5Å), (B) Class II (width diameter 371±4.5Å), (C) Class III (width diameter 380±4.5Å), and (D) Class IV (width diameter 389±4.5Å).

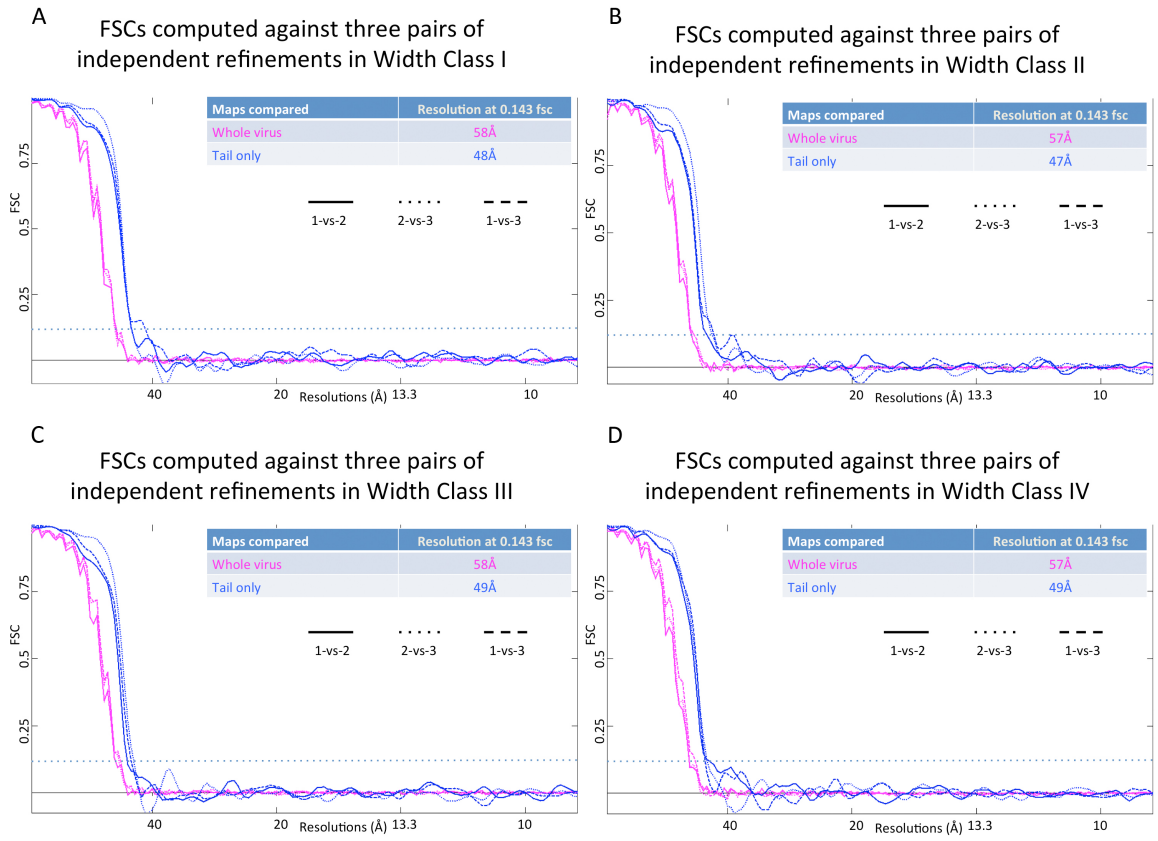

Figure S8. FSCs calculated among the three independent refinements for each width group. (A) For Class I, FSCs compared against three pairs of independent refinements (1-vs-2 as solid line, 2-vs-3 as dotted line, 1-vs-3 as dashed line). (B) For Class II, FSCs compared against three pairs of independent refinements. (C) For Class III, FSCs compared against three pairs of independent refinements. (D) For Class IV, FSCs compared against three pairs of independent refinements. The magenta curve represents the comparison of the whole virus maps including the lemon body. The blue curve is the comparison of only the tail part. The tables summarize the resolution values for the FSC curves at 0.143 cutoff threshold.

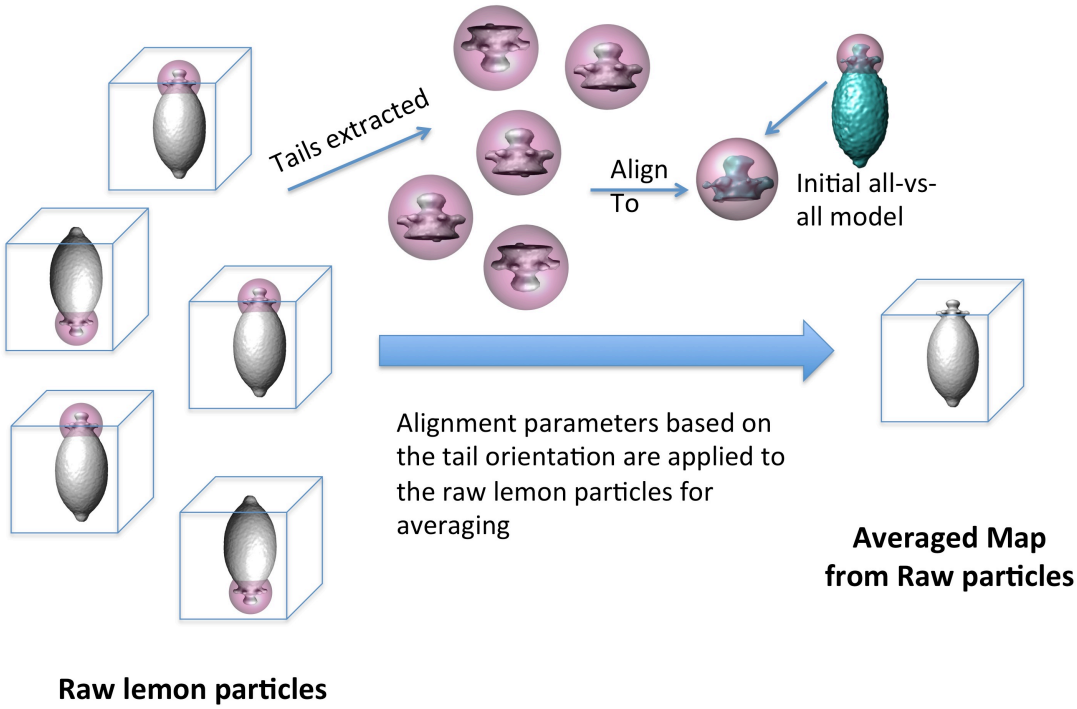

Figure S9. Diagram illustrating the focused alignment on the tail only. Tails for all the raw lemon particles were extracted and refined against the tail extracted from initial all-vs-all model. Alignment parameters based on the tail orientation were applied to the raw lemon particle. Then the aligned raw lemon particles would be averaged to generate the final map.

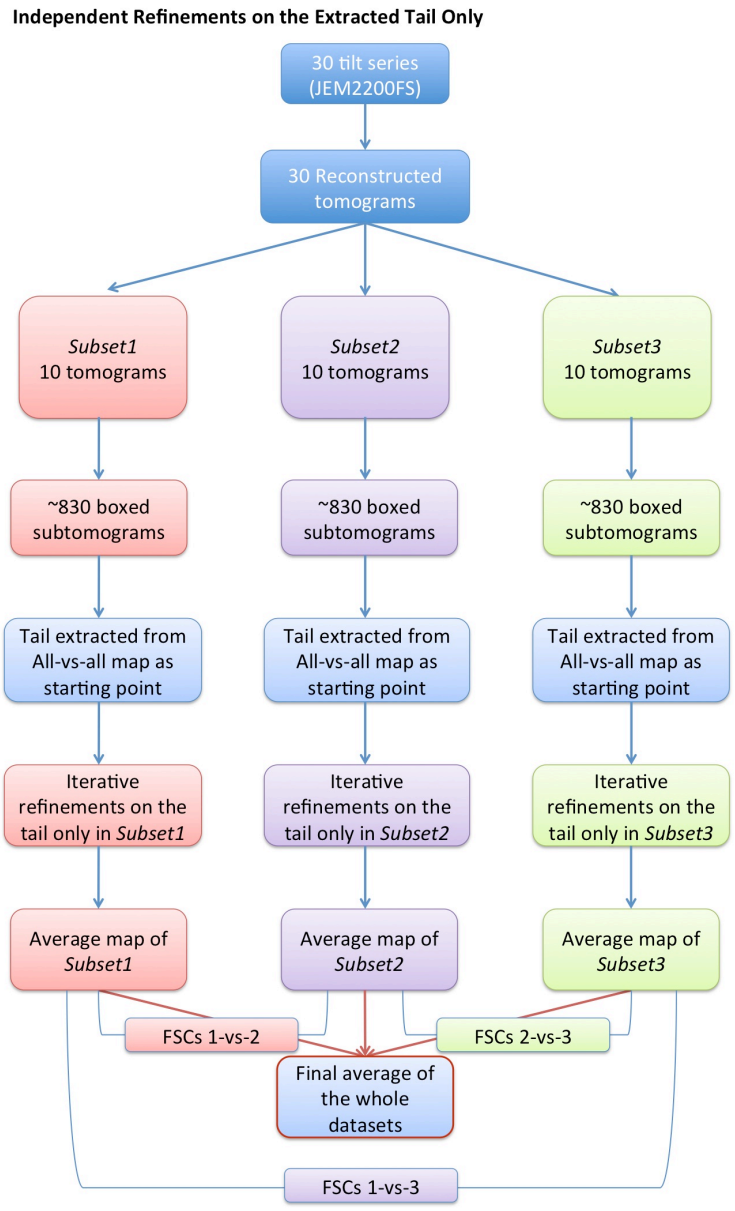

Figure S10. Workflow for the subtomogram refinement. The process is shown as a workflow to represent the three independent refinements. The three subsets were split according to the month the tomogram data were collected, namely Subset1 colored in red, Subset2 in purple and Subset3 in green. The iterative refinements were done independently within each subset using improved averages for the next iteration. FSCs calculated for each pair of the three subsets were obtained.

A

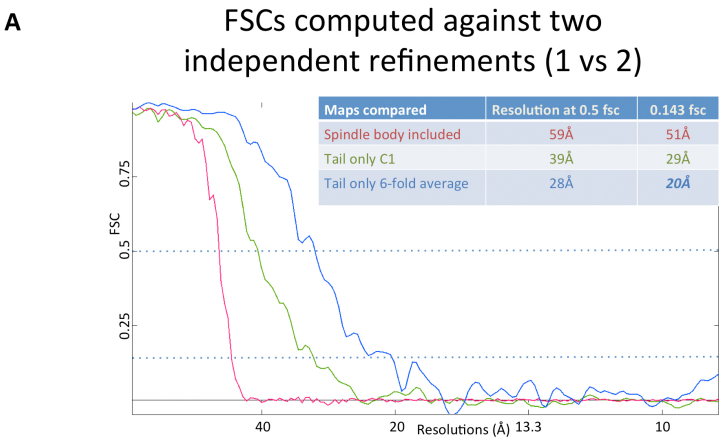

B

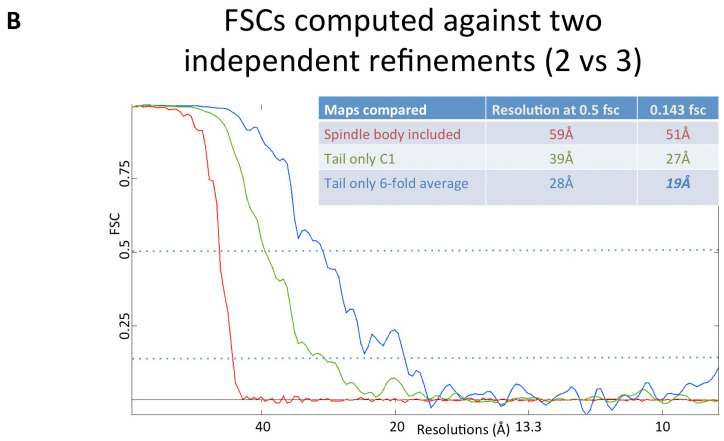

C

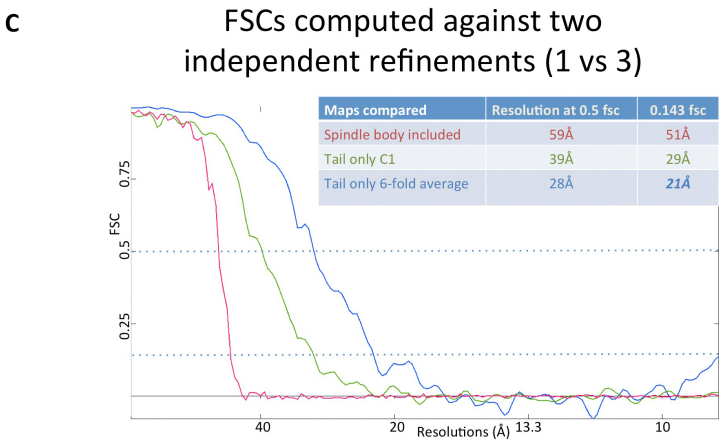

Figure S11. FSCs calculated among the three independent refinements. (A) FSCs compared against two independent refinements 1-vs-2. (B) FSCs compared 2-vs-3. (C) FSCs compared 1-vs-3. The red curve represents the comparison of the whole virus maps including the capsid. The green curve is the comparison between only the tail part. The blue curve is compared with six-fold averaged tail part. The tables summarize the resolution values for the curves at 0.5 and 0.143 cutoff thresholds.

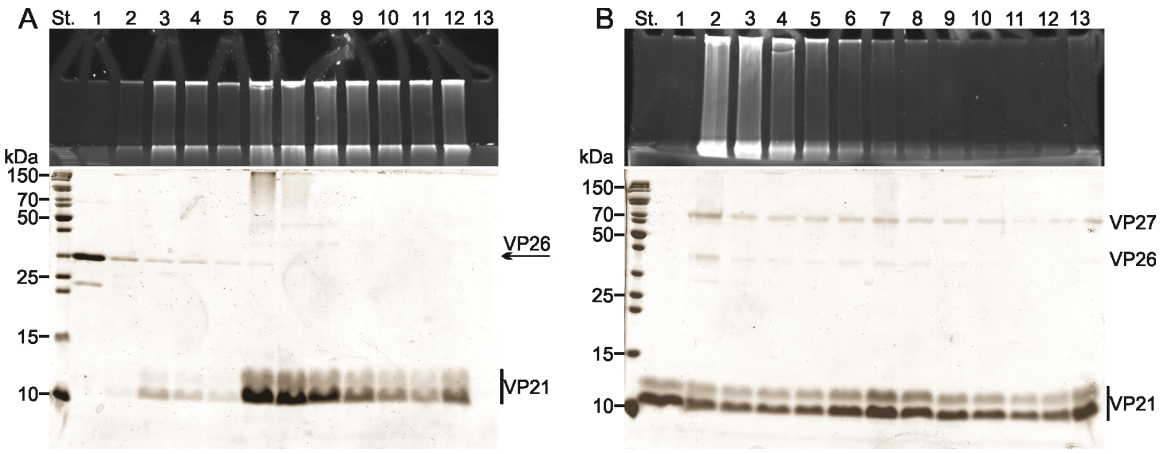

Figure S12. Proteinase K and NP-40 treatment of His1 virions. The treated virions were analysed by rate zonal centrifugation, after which the gradient was fractionated. (A) Virions treated with proteinase K (0.2 mg/ml) at low salinity at 37°C for 90 min. Arrow indicates proteinase K bands. (B) Virions treated with 1% (v/v) NP-40 at RT at low salinity for 90 min.

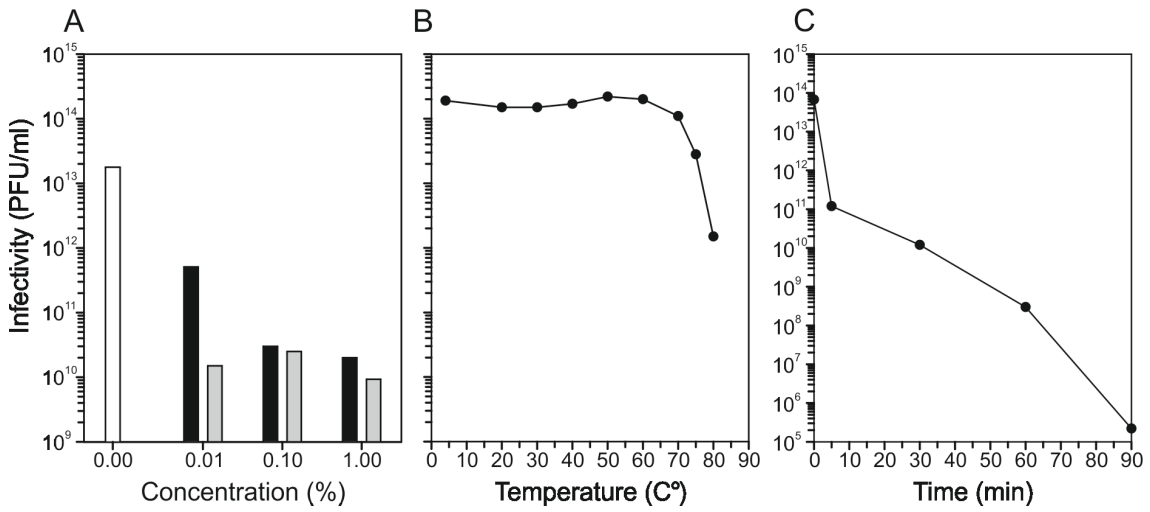

Figure S13. Infectivity of His1 virions after detergent and temperature treatments. (A) '2× purified' His1 virions were treated with Tx-100 (black bars) or NP-40 (grey bars) and incubated at low salinity at RT for 90 min, after which the infectivity was determined by plaque assay. White bar represents untreated virions. (B) '2× purified' His1 virions incubated at low salinity at different temperatures for 5 min. The y-axis in A and B is the same. (C) '2× purified' His1 virions incubated at low salinity at 80°C for 5-90 min. The first time point indicates untreated virions.

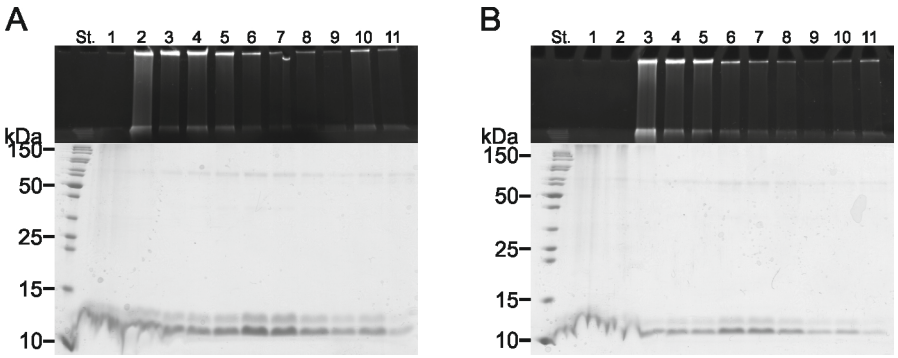

Figure S14. NP-40 treatment of His1 virions. The treated virions were analysed by rate zonal centrifugation, after which the gradient was fractionated. (A) Virions treated with 4% (v/v) NP-40 at low salinity at RT for 90 min. (B) Virions treated with 6% (v/v) NP-40 at low salinity at RT for 90 min.

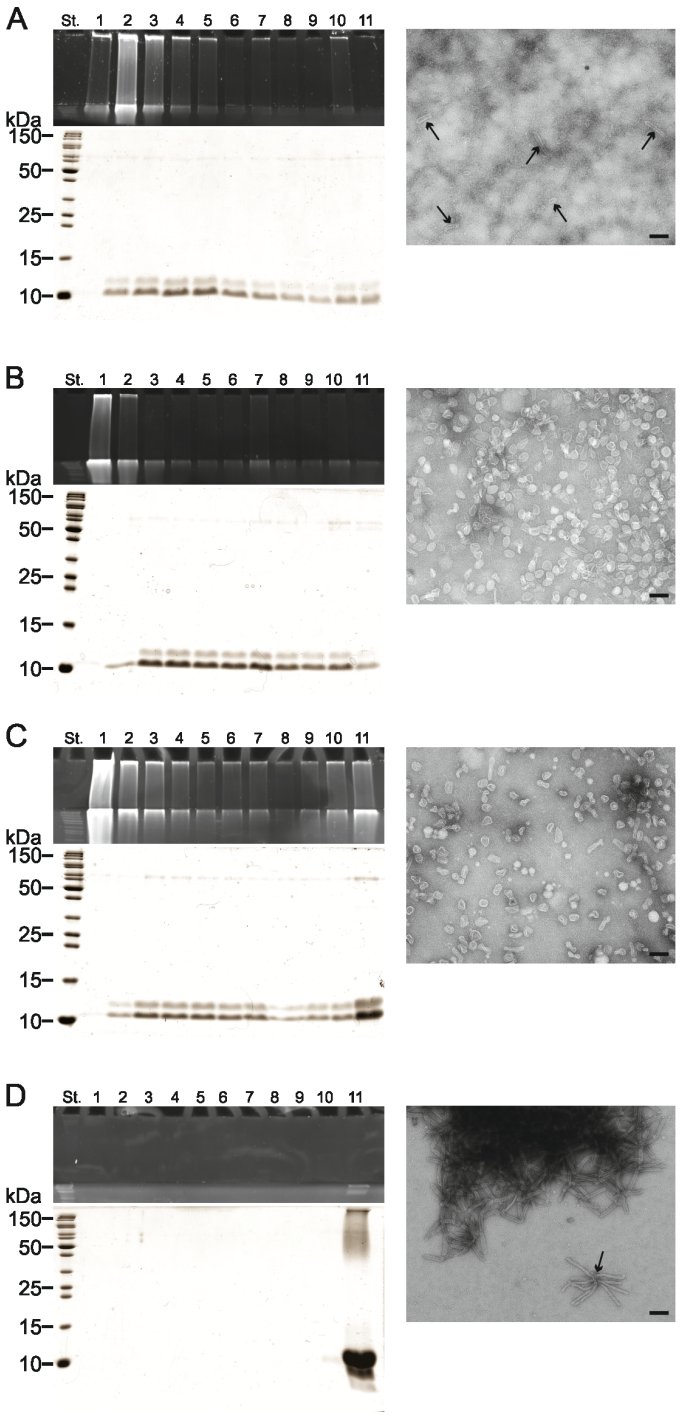

Figure S15. Octyl-β-D-glucopyranoside, HCl and chloroform treatment of His1 virions. The treated virions were analysed by rate zonal centrifugation, after which the gradient was fractionated. In addition, electron micrographs of the treated samples stained with uranyl-acetate are shown (scale bar, 100 nm). (A) Virions treated with 100 mM octyl-β-D-glucopyranoside at low salinity at RT for 60 min. Arrows indicate tubes of different sizes. (B and C) Virions treated with 5% (v/v) chloroform at low salinity at RT for 90 min. B shows the analysis of the aqueous and C shows the analysis of the organic phase. (D) Virions treated with 1.5% (v/v) HCl at low salinity at 75°C for 120 min. Arrow indicates a rosette formed by rod-like tubes.

Table S1. Summary of His1 dissociation experiments.

No.	Treatments / conditions	Infectivity (PFU/ml)[a]	DNA release (+/-)	Soluble VP21	Notes[b]
1	Untreated particles	3.1×10^{13} (100%)	-	-	
	Proteases				
2	Proteinase K (0.2 mg/ml); 10-fold diluted His1 buffer; 90 min at 37°C	7.8×10^{10} (<1%)	-	-	No major digestion products were observed. The treated particles sedimented like the untreated virions.
3	Trypsin (0.2 mg/ml); 10-fold diluted His1 buffer; 90 min at 37°C	2.4×10^{10} (<1%)	-	-	
4	Bromelain (0.2 mg/ml); 10-fold diluted His1 buffer; 90 min at 37°C	7.2×10^{9} (<1%)	-	-	
	pH				
5	1, 2 and 5% (v/v) HCl[c]; 10-fold diluted His1 buffer; 60 min at RT	6.0×10^{3} (<1%)[d]	-	-	The treated particles sedimented like the untreated virions. After treatment with 1% HCl, the majority of the particles were lemon-shaped but some were elongated.
6	50 mM NaOH; 10-fold diluted His1 buffer; 60 min at RT	3.4×10^{9} (<1%)	+	-	Empty tube-like particles were observed with uniform S-values and sedimenting slower than the untreated virions.
	Detergents				
7	0.1% (v/v) Tween; 10-fold diluted His1 buffer; 90 min at RT	5.4×10^{13} (100%)	-	-	The treated particles sedimented like the untreated virions.

8	0.1% (v/v) Tx-100; 10-fold diluted His1 buffer; 90 min at RT	9.6×10^{10} (<1%)	+	-	Empty tube-like particles were observed with uniform S-values and sedimenting slower than the untreated virions. One half of VP27 was observed on the top of the gradient and the other half associated with the empty particles.
9	0.01% (v/v) NP40; 10-fold diluted His1 buffer; 90 min at RT	2.5×10^{10} (<1%)	+	-	
10	0.1-6.0% (v/v) NP40; 10-fold diluted His1 buffer; 90 min at RT	nd	+	+	With an increasing NP40 concentration, VP21 became partially soluble but no more than half of the protein was on the top of the gradient. Empty particles with highly variable S-values were observed.
11	100 mM octyl-β-D-glucopyranoside; 10-fold diluted His1 buffer; 60 min at RT	6.9×10^{4} (<1%)	+	-	Empty tube-like particles with highly variable S-values were observed.
12	0.5% (v/v) SDS; 10-fold diluted His1 buffer; 90 min at RT	$<10^{4}$ (<1%)	+	+	Both forms of VP21 were solubilised.
	Temperature				
13	Freezing -20°C and thawing; His1 buffer	3.8×10^{13} (100%)	-	-	The treated particles sedimented like the untreated particles.
14	Freezing -80°C and thawing; His1 buffer	2.7×10^{13} (87%)	-	-	
15	80°C; 10-fold diluted His1 buffer; 5 and 90 min	5.1×10^{10} (<1%)[e]	+	-	Empty tube-like particles were observed with uniform S-values and sedimenting slower than the untreated virions. A minor

					fraction of the empty tubes still contained bound DNA. Minor aggregation of DNA and proteins was observed.
16	Boiling; 10-fold diluted His1 buffer; 5 and 10 min	2.6×10^{10} (<1%)[f]	+	-	Empty tube-like particles were observed with uniform S-values and sedimenting slower than the untreated virions. Minor aggregation of DNA and proteins was observed.
	Chaotropic agents				
17	3 M urea; 10-fold diluted His1 buffer; 60 min at RT	2.5×10^{13} (81%)	-	-	The treated particles sedimented like the untreated virions.
18	3 M guanidine hydrochloride; 10-fold diluted His1 buffer; 60 min at RT	2.4×10^{13} (77%)	-	-	
	Solvents				
19	5% (v/v) chloroform; 10-fold diluted His1 buffer; 90 min at RT	4.4×10^{5} (<1%)	+	-	Empty pleomorphic particles with highly variable S-values were observed. Minor aggregation of DNA and proteins was observed.
20	5% (v/v) ethanol; 10-fold diluted His1 buffer; 90 min at RT	2.9×10^{13} (94%)	-	-	The treated particles sedimented like the untreated virions.
	Combination treatments				
21	1) 80°C; 10-fold diluted His1 buffer; 90 min → 2) proteinase K (0.2 mg/ml); 10-fold diluted His1	nd	+	-	Particles incubated at 80°C at low salinity aggregated after the proteinase K treatment. No major digestion was

	buffer; 90 min 37°C				observed.
22	1) 80°C; 10-fold diluted His1 buffer; 90 min → 2) trypsin (0.2 mg/ml); 10-fold diluted His1 buffer; 90 min 37°C	nd	+	-	The trypsin or bromelain treatments did not affect the solubility of the particles incubated at 80°C at low salinity. No major digestion was observed.
23	1) 80°C; 10-fold diluted His1 buffer; 90 min → 2) bromelain (0.2 mg/ml); 10-fold diluted His1 buffer; 90 min 37°C	nd	+	-	
24	1.5% (v/v) HCl[g]; 10-fold diluted His1 buffer; 120 min at 75°C	$<10^4$ (<1%)	+	-	Highly aggregative, empty tube-like particles were observed. The majority resembled those of dissociations no. 6, 8, 9, 14, and 15, but a few were thinner rod-like particles. The lipid-modified form of VP21 was digested as previously reported (Pietilä et al., 2012).

[a] Blue shading indicates that more than 50% of virus particles remained infective.
[b] The dissociation products were analysed by SDS-PAGE and negative-staining TEM.
[c] 1, 2 and 5% (v/v) HCl ≈ 0.3, 0,7 and 1.6 M HCl.
[d] The infectivity was determined after the 1% HCl treatment.
[e] The infectivity was determined after the 5 min treatment.
[f] The infectivity was determined after the 5 min treatment.
[g] 1.5% (v/v) HCl ≈ 0.5 M HCl
nd, not determined.

Pietilä, M.K., Atanasova, N.S., Oksanen, H.M., and Bamford, D.H. (2012). Modified coat protein forms the flexible spindle-shaped virion of haloarchaeal virus His1. Environmental microbiology.

Moive S1. Tilt series of His1 virion.

Moive S2. Reconstructed tomogram of His1 virion.

Movie S3. Lemon-shaped Archaeal Virus His1 Single-Particle Cryo-ET.

Moive S4. Tilt series of empty His1 tube.

Moive S5. Reconstructed tomogram of empty His1 tube.